

# Preparation of macroporous poly (2-hydroxyethyl) methacrylate with interconnected porosity

I. C. STANCU<sup>a,b\*</sup>, P. LAYROLLE<sup>c</sup>, H. LIBOUBAN<sup>a</sup>, R. FILMON<sup>a</sup>,  
G. LEGEAY<sup>c</sup>, C. CINCUB<sup>b</sup>, M. F. BASLÉ<sup>a</sup>, D. CHAPPARD<sup>a</sup>

<sup>a</sup>INSERM, EMI 0335, LHEA- Faculté de Médecine, 49045 ANGERS Cédex - France

<sup>b</sup>Department of Macromolecular Chemistry, Industrial Chemistry Faculty, University Politehnica, Bucharest, Romania

<sup>c</sup>CTM, Technopole Université, 72000 LE MANS, France

The design of a macromolecular bone graft with interconnected macroporosity represents a major challenge in the field of orthopaedic biomaterials. Such a synthetic graft would combine the biocompatibility and the biomechanical behavior with a micro-architecture allowing the osteoconduction through the colonization of the implant by bony cells and blood vessels. Macroporous pHEMA blocks were obtained by polymerizing 2-hydroxyethyl methacrylate around polystyrene beads of four diameters (600, 800, 1200, 1600  $\mu\text{m}$ ). X-ray microtomography (microCT) and scanning electron microscopy were used to evaluate the porosity and the interconnectivity. Porosity did not differ whatever the size of the beads used as porogen. Porosity was in the range of 58-66%, close to that of calf trabecular bone, a material used for preparing bone xenografts. Chromatographic analysis was performed in order to check the presence of residual monomer. The biomechanical characteristics of these porous materials were measured in compression and appeared close to those of calf bone used for xenografts.

(Received May 30, 2007; accepted June 27, 2007)

Keywords: Biomaterial, Macroporous methacrylate, X-ray microtomography, SEM

## 1. Introduction

The design of synthetic biomaterials for bone grafts represents one of the most active areas in the orthopaedic materials field. Trabecular bone is a natural composite material, with a porous microarchitecture adapted to high mechanical stresses. The presence of the interconnected porosity allows a better diffusion and circulation of fluids inside the material, facilitated invasion by bone cells and blood vessels (during bone remodelling) and facilitated escape of young haematological blood cells (from the marrow to the blood vessels). From this point of view, a macroporous synthetic biomaterial with interconnected pores would be suitable as bone graft because of the enhanced implant incorporation through rapid vascularization and bone ingrowth [1-4]. These reasons explain why the design of such macroporous matrices represents a major challenge in the design of orthopaedic biomaterials.

However, porosity should not hamper the biomechanical properties of the biomaterial which have to present performances similar to bone.

## 2. Material and methods

All reagents were purchased from Sigma-Aldrich (St-Quentin-Fallavier, France). HEMA was purified by distillation under reduced pressure, at 47°C and 2.6 Pa. Benzoyl peroxide (BPO), N,N-dimethyl-p-toluidine (N,N-DMpT) and dichloromethane were used without further purification. Polystyrene (average Mw ca 230 000,

average Mn ca 140 000) and poly(vinyl alcohol) (87-89% hydrolyzed, average Mw: 31 000 – 50 000) were used as received. Blocks of cancellous bone were prepared from calf femoral condyles [11]. These bony blocks are currently used as xenograft because calf bone has exactly the same properties than human bone on a microarchitectural and biomechanical point of view.

### 2.1 Preparation of polystyrene beads

The solvent-evaporation technique was used to prepare polystyrene beads by using a modification of the method described by Kentepozidou and Kiparissides [12]. Briefly, 70 ml of dichloromethane (containing 10% w/v of polystyrene) were dispersed by gentle dropping in 500 ml of 0.01% (w/v) poly(vinyl alcohol) aqueous solution. The emulsion was formed by stirring using an anchor-type propeller at 500 rpm at ambient temperature. Stirring was maintained for 8 hours, in order to assure solvent evaporation from droplets, and subsequent solidification of polystyrene beads. Four diameters (600, 800, 1200, 1600  $\mu\text{m}$ ) beads were sieved for further use as porogens. The mean diameter of the beads was verified by scanning electron microscopy (SEM).

### 2.2 Preparation of macroporous pHEMA blocks

Polystyrene beads (600-1000 mg) were transferred into 10 ml polyethylene tubes. Five hundred mg of HEMA were maintained under nitrogen gas bubbling for 15 minutes. Polymerization was initiated with 0.125% (w/v) BPO and accelerated with N,N-DMpT 0.3% (v/v) and the

mixture was poured into the polyethylene tubes containing the polystyrene beads. Six samples were prepared for each size of bead. Six additional blocks of pHEMA were bulk-polymerized without porogen beads using the same method and served as controls.

All blocks (either containing polystyrene beads or not) have been considered totally polymerized after 8 hours at room temperature. Three blocks from each series of polystyrene beads and the corresponding control samples were demolded eight hours after the onset of polymerization and the others were collected after 27 days waiting period at room temperature. The porogen beads were dissolved during three days in 35 ml dichloromethane (a non-solvent for pHEMA) which also extracted residual monomer molecules. This solution was used to evaluate also the level of unreacted monomer by gas phase chromatography. The blocks were then dried at 40°C for 48 hours.

### 2.3 Evaluation of porosity and interconnectivity

The 3D microarchitecture and the porosity were analysed by microtomography as previously reported [10]. Briefly, the porous blocks were fixed on brass stubs and analysed with a Skyscan 1072 X-ray computed microCT (Skyscan – Aartselaar, Belgium). They were examined at magnification of 26 (a pixel corresponding to 11.41 µm) with the cone beam mode. For each block, 208 projection images were acquired every 0.90° rotation and stored in the tif format. They were converted to a stack of 2D transverse sections that were coded on 8 bits, 256 gray levels and stored as bmp files. After an interactive threshold, 3D virtual models of the blocks were generated with a surface program (ANT, release 2.2.5 – Skyscan-Aartselaar, Belgium). The program offers facilities for all types of model rotations, displacements, lightening effects and colouring of the desired structures. Both components of the blocks (i.e., the pores and the polymeric matrix) could be visualized and measured separately. The reference volume was the volume of the block itself (TV, in mm<sup>3</sup>). The 3D porosity (PoV/TV, expressed in %) was directly measured on the CtAn software. Porosity of calf bone was measured similarly on eight samples.

The porosity of blocks was also observed directly by scanning electron microscopy (SEM) on a field emission microscope JEOL 6301 (JEOL, France), equipped with an energy dispersive X-ray microanalysis machine (Link-ISIS, Oxford, UK). Before analysis, blocks were covered by a thin carbon coating (1 nm thick) deposited by sputtering on a MED 020 Baltec (Balzers, Liechtenstein).

### 2.4 Residual HEMA monomer analysis

For each series of polystyrene beads, the dichloromethane used to dissolve the polystyrene beads had also extracted the residual monomer. The unreacted HEMA was dosed by gas phase chromatography (GPC, Perkin-Elmer, Model Autosystem). GPC analyses were performed with a nitrogen gas flow of 40 ml/min at 15 Psi, an injection loop of 1 µl heated at 250 °C, a capillary column Simplicity-5 (length 30 m, internal diameter 0.25

mm) maintained at 280 °C and FID detector at 300 °C. A standard calibration line was made with 236.34 mg HEMA in 25 ml CH<sub>2</sub>Cl<sub>2</sub> (9.454 g/l) then diluted to 2:25 and again between 1:10 (0.076 g/l) to 4:10 (0.310 g/l) in CH<sub>2</sub>Cl<sub>2</sub>. The same standard injected in triplicate gave reproducibility for measurements of 0.4 %. Samples obtained after polymerization and lasting time of 3 and 30 days were injected in the GPC using the same conditions. The residual HEMA monomer was expressed as a percentage of total HEMA used for the polymerization.

### 2.5 Biomechanical analysis

The macroporous and dense pHEMA blocks were tested for their resistance in compression. The pHEMA cylinders with a diameter of 9 mm were cut by using a diamond saw in order to get parallel faces at a distance of 15 mm. The mechanical tests were performed in compression mode with a bench (MTS, model DY 25) using a load cell of 100 daN at a strain rate of 1 mm/min. The load was continuously recorded as strain increased. The maximum stress was determined at a flow threshold of about 5 %. Compressive strength was expressed in MPa (maximum load in N/section in m<sup>2</sup>). Samples of cancellous bone were measured in the same conditions for comparison.

### 2.6 Statistical analysis

Statistical study was performed using the Systat statistical software release 10.0 (SPSS, Chicago, Ltd). All data were expressed as mean and standard error of the mean. Pearson correlations were used to examine the relationships between variables. Differences were evaluated by analysis of variance (ANOVA) with Fischer's probability least significant difference (PLSD) post-hoc test. Differences were considered significant when  $p < 0.05$ .

## 3. Results

After sieving, bead populations were homogeneous, as shown in Fig. 1. After polymerization and dissolution of porogen beads, pHEMA blocks with different porosities were obtained.

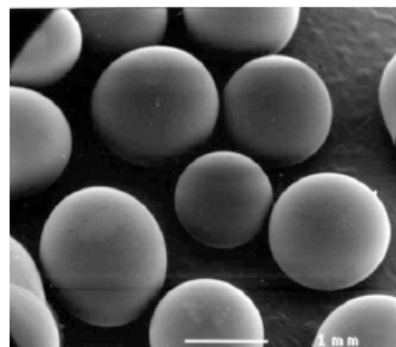


Fig. 1. SEM micrographs of polystyrene beads used as porogen. Diameter = 1600 µm.

### 3.1 Porosity and connectivity

The porogen was highly soluble in the chosen solvent and completely dissolved within 2-3 days. The use of polystyrene beads as porogen allowed the formation of a homogenous dense network of interconnected spherical pores, distributed in all polymeric blocks. The size of the pores, determined by microCT, was in the expected values (i.e., similar to the diameter of polystyrene particles used as porogen).

The microtomographic appearance of the four types of blocks is illustrated in Figure 2. Table 1 presents the microCT measurements for each pHEMA block. The porosity of the whole series of blocks was in the range of 58-66%. Porosity was not significantly influenced by the dimensions of the beads used to prepare the samples. Porosity was not modified by prolonged storage since the two time series did not differ significantly.

SEM observations of the blocks confirmed the interconnection of the pores in the tangential contact area between beads (Figure 3). Although SEM allowed a more precise visualization of the interconnectivity, it provides only a partial 3D description of the polymer blocks which was limited by the depth of field.

### 3.2 Residual monomer elimination

After an 8 hour polymerization time, the blocks had hardened but the amount of unreacted monomer remained at a high level with a maximum value of 14.44% for blocks with the highest pore size. No clear linear relationship could be observed between the amount of residual monomer and the size of the beads ( $r = 0.40$ ,  $p = 0.18$ ). When monomer was extracted from the blocks at distance from the hardening period, the amount of non-reacted HEMA appeared to decrease considerably (Figure 4). However, no significant relationship could be observed with the size of the beads at that time ( $r = 0.20$ ,  $p = 0.53$ ). The amount of unreacted monomer was significantly higher in any type of porous blocks than in the non-porous ones used as controls which contained an average amount of only  $3.15 \pm 0.65$  % after 8 hours, and  $0.3 \pm 0$  % after 27 days. This indicates that the presence of the polystyrene beads used as porogen have partially affected the homogeneity of the polymerization mixtures since all the experimental conditions were kept constant during the preparation of this series of blocks.

### 3.3 Biomechanical analysis

Table 2 presents the compressive strength and the strain obtained for each type of samples as average of three measurements. Biomechanical testing failed to identify a significant relationship between the diameter of the pores and the mechanical characteristics of the blocks. No significant differences were observed between the series indicating that the mechanical strength was not modified by the dimensions of the pores (strain:  $F = 0.205$ ;

$p = 0.89$ ; strength:  $F = 1.31$ ,  $p = 0.33$ ). However, whatever the pore size, the mechanical strength was lower than compared to blocks of polymer without porosity. The biomechanical analysis of calf cancellous bone showed performed in the same conditions provided significantly lower values.

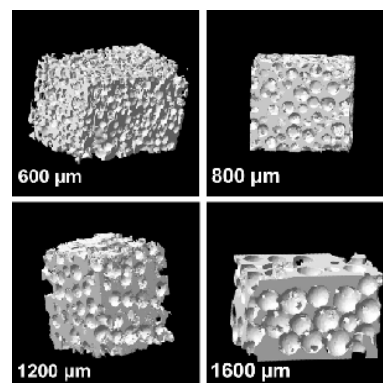


Fig. 2. MicroCT appearance of the four types of porous polymer blocks obtained by using polystyrene beads of different diameters; a) 600, b) 800, c) 1200 and d) 1600  $\mu\text{m}$ .

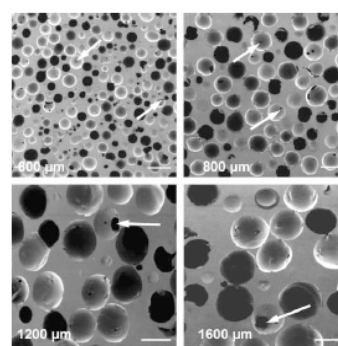


Fig. 3. SEM appearance of the longitudinal sections of the macroporous pHEMA blocks. The arrow points to an interconnection area when two beads were in contact. The diameters of the pores are: 600  $\mu\text{m}$ ; 800  $\mu\text{m}$ ; 1200  $\mu\text{m}$ ; 1600  $\mu\text{m}$ .

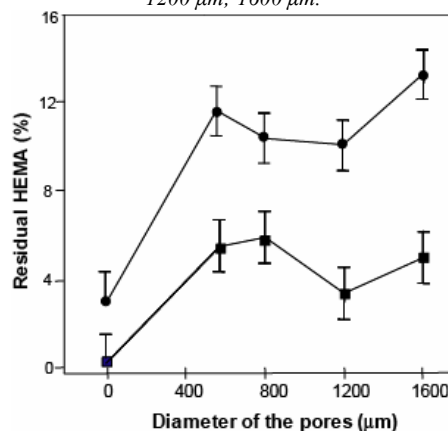


Fig. 4. Evaluation of residual monomer in macroporous pHEMA blocks. ● after dissolution of the porogen, 8 hours after the end of polymerization; ■ after dissolution of the porogen, 27 after the end of

polymerization.

Table 1. MicroCT analysis of the porosity of pHEMA blocks (prepared with 4 different porogens) and calf trabecular bone.

Pore diameter (µm)	Porosity after 8 hours (%)	Porosity after 27 days (%)	p
600	60.1 ± 3.9	64.1 ± 3.3	NS
800	66.2 ± 0.5	63.5 ± 1.2	NS
1200	61.7 ± 4.9	61.8 ± 1.0	NS
1600	58.6 ± 2.0	65.1 ± 0.6	NS
Trabecular bone	73.9 ± 8.1		

Table 2. Biomechanical behaviour of the polymer blocs and calf trabecular bone (mean ± SD).

Diameter of the pores (µm)	Compressive stress (MPa)	Strain (%)
0	45.00 ± 4.8	9.30 ± 0.85
600	8.46 ± 0.56	5.83 ± 0.54
800	8.83 ± 0.68	5.86 ± 0.12
1200	9.40 ± 0.21	5.86 ± 0.50
1600	8.00 ± 1.14	5.60 ± 0.29
Trabecular bone	7.10 ± 1.28	5.00 ± 0.71

#### 4. Discussion

There is growing scientific interest in developing porous materials for different biomedical applications and specially in the orthopaedic area [9,13-26]. Several methods have been developed for obtaining porous polymers: heat-compressing of fiber mesh, emulsion freeze drying [27], thermally induced phase separation [19,20], solvent casting/salt leaching [13,14], phase separation [15,27], gas foaming [17,19,28], water soluble porogens [10,29]. The interest in these biomaterials consists in their rapid invasion by vascular sprouts and high density of cells promoting the osseointegration of the implant. Their major disadvantage is the lack of control of pore size and the difficulty to obtain and control interconnection of the pores. It has previously been showed that interconnectivity is essential for cell invasion and vascularization [18,24]. However, polymer sponges obtained by the above methods are not mechanically appropriate for orthopaedic applications. Lin et al., described other problems associated with the use of these methods [25]. For example, solvent casting/particulate leaching is limited to thin films or wafers, thermally induced phase separation creates foams with lack of interconnectivity, gas foaming produces open and closed pores with a non porous envelope.

In this context, the preparation of a controlled interconnected macroporous matrix based on pHEMA is a difficult and important challenge. MicroCT is a very

interesting tool suitable for quantitative microanalysis of bone and biomaterials even in the absence of a mineral phase [10,30-32].

We have chosen to create interconnected spherical pores networks by dissolution of porogen particles (with a controlled size) after bulk polymerization of HEMA. This technique was already used for water-soluble porogens such as urea, sucrose crystals and sucrose-glucose fibers but the amount of polymer material in the porous block was much higher than the trabecular bone volume in a cancellous space [10]. In order to reduce the amount of polymer (or conversely to increase porosity) the use of polystyrene beads as a porogen could represent a suitable alternative. Polystyrene is highly soluble in several organic solvent and do not interact with HEMA during polymerization. In addition, the porogen is hydrophobic while pHEMA is highly hydrophilic. The porosity of pHEMA blocks obtained with polystyrene beads remained somewhat higher than in calf trabecular bone but very close to the normal values reported in normal human young males [33]. The biomechanical behavior was superior to that of calf trabecular blocks used in this series. However, these values are very similar to those obtained with commercial bovine xenografts: Endobon® (Merck Biomaterial France – Valence) has 450 µm pore diameter, 50-60% porosity; Luboc® (Ost Development, Clermont-Ferrand, France) has pores ranging from 200-1500 µm in diameter with a mean porosity of 81%.

Recent investigations have revealed that microarchitecture of trabecular bone is an important component of bone strength either when determined experimentally [34] or clinically [35]. The porous architecture obtained by dissolving the polystyrene beads provides **an interconnected porosity** on the contact areas between beads. Such architectures are **very similar to the theoretical models** proposed by biomechanical specialists to mimic trabecular architecture [36]. The design of these polymer blocks interfered with the amount of residual monomer (whatever the size, beads were associated with the lowest amount of residual monomer) but did not appear to influence mechanical properties.

#### Acknowledgements

This work has been made possible with the help of the SOCRATES-ERASMUS European Community Program. Grants were obtained from the Contrat de Plan Etat – Région “Pays de la Loire”.

#### References

- [1] T.E. Gredga, J.E. Zins, T.W. Bauer, *Plast. Reconstr. Surg.* **84**, 245-249 (1989).
- [2] H. Schliephake, D. Klosa, F.W. Neukam, *Int. J. Oral Maxillofac. Implants* **6**, 168-176 (1991).
- [3] H. Schliephake, F.W. Neukam, D. Klosa, *Int. J. Oral Maxillofac. Implants* **20**, 53-58 (1991).
- [4] D.C. Tancred, B.A. McCormack, A.J. Carr,

- Biomaterials **19**, 2303-2311 (1998).
- [5] J. P. Monthéard, M. Chatzopoulos, D. Chappard, J. Macromol. Sci. Macromol. Rev. **32**, 1-34 (1992).
- [6] J.P. Monthéard, J. Kahovec, D. Chappard, In: Arshady R editors, "Desk references of functional polymers; Synthesis and applications", Washington D. C., American Chemical Society, 699-717 (1997).
- [7] R. Filmon, D. Chappard, J. P. Montheard, M. F. Baslé, Cells Mater. **6**, 11-20 (1996).
- [8] R. Filmon, M.F. Baslé, H. Atmani, D. Chappard, Bone **30**, 152-88 (2002).
- [9] C. Schiraldi, A. D'Agostino, A. Oliva, F. Flamma, A. De Rosa, A. Apicella et al., Biomaterials **25**, 3645-53 (2004).
- [10] R. Filmon, N. Retailleau-Gaborit, F. Grizon, M. Galloyer, C. Cincu, M.F. Baslé et al., J. Biomater. Sci. Polymer Edn. **13**, 1105-1117 (2002).
- [11] D. Chappard, C. Fressonnet, C. Genty, M.F. Baslé, A. Rebel, Biomaterials **14**, 507-512 (1993).
- [12] A. Kentepozidou, C. Kiparissides, J. Microencapsul. **12**, 627-638 (1995).
- [13] A.G. Mikos, G. Sarakinos, S.M. Leite, J.P. Vacanti, R. Langer, Biomaterials **14**, 323-330 (1993).
- [14] A.G. Mikos, A.J. Thorsen, L.A. Czerwonka, Y. Bao, R. Langer, D.N. Winslow et al., Polymer **35**, 1068-1077 (1994).
- [15] H. Lo, S. Kadiyala, S.E. Guggino, K.W. Leong, J. Biomed. Mater. Res. **30**, 475-484 (1996).
- [16] V.I. Lozinsky, F.M. Plieva, Enzyme Microb. Technol. **23**, 227-242 (1998).
- [17] L.D. Harris, B.S. Kim, D.J. Mooney, J. Biomed. Mater. Res. **42**, 396-402 (1998).
- [18] C.N. Cornell, J.M. Lane, Clin. Orthop. **355S**, 267-73 (1998).
- [19] Y.S. Nam, T.G. Park, Biomaterials **20**, 1783-90 (1999).
- [20] Y.S. Nam, T.G. Park, J. Biomed. Mater. Res. **47**, 8-17 (1999).
- [21] C.J. Spaans, V.W. Belgraver, O. Rienstra, J. H. de Groot, R.P. Veth, A.J. Pennings, Biomaterials **21**, 2453-2460 (2000).
- [22] Y.S. Nam, J.J. Yoon, T.G. Park, J. Biomed. Mater. Res. **53**, 1-7 (2000).
- [23] J.A. Burdick, D. Frankel, W.S. Dernel, K.S. Anseth, Biomaterials **24**, 1613-1620, (2003).
- [24] S. Kujala, J. Ryhanen, A. Danilov, J. Tuukkanen, Biomaterials **24**, 4691-4697 (2003).
- [25] A.S. Lin, T.H. Barrows, S.H. Cartmell, R.E. Guldberg, Biomaterials **24**, 481-9 (2003).
- [26] V. J. Chen, P.X. Ma, Biomaterials **25**, 2065-2073 (2004).
- [27] K. Whang, C.H. Thomas, K.E. Healy, G.A. Nuber, Polymer **36**, 837-842 (1995).
- [28] D.J. Mooney, D.F. Baldwin, N.P. Suh, J.P. Vacanti, R. Langer, Biomaterials **17**, 1417-1422 (1996).
- [29] H. S. Zaki, I. L. Kamel, J. Dent. Res., **55**, 272-280 (1976).
- [30] S.V. Jaecques, H. Van Oosterwyck, L. Muraru, T. Van Cleynenbreugel, E. De Smet, M. Wevers et al. Biomaterials, **25**, 1683-1696 (2004).
- [31] S. Cartmell, K. Huynh, A. Lin, S. Nagaraja, R. Guldberg, J. Biomed. Mater. Res., **69A**, 97-104 (2004).
- [32] D. Chappard, S. Blouin, H. Libouban, M.F. Baslé, M. Audran, Microsc. Anal. **19**, 17-19, (2005).
- [33] P. Courpron, P. Meunier, C. Edouard, J. Bernard, J.P. Bringuier, G. Vignon, Rev. Rhum. Mal. Osteoartic. **40**, 469-483 (1973).
- [34] C.H. Turner, Osteoporos Int., **13**, 97-104 (2002).
- [35] E. Legrand, D. Chappard, C. Pascaretti, M. Duquenne, S. Krebs, Y. Simon et al., J. Bone Miner. Res. **15**, 13-19 (2000).
- [36] G.H. van Lenthe, R. Huiskes, J. Biomech. **35**, 1191-1197 (2002).

\*Corresponding author: Izabela.Stancu@UGent.be